Chem Soc Rev

Cite this: *Chem. Soc. Rev.*, 2012, **41**, 7354–7367

www.rsc.org/csr

TUTORIAL REVIEW

A comprehensive comparison of transition-metal and actinyl polyoxometalates†

May Nyman‡*[a] and Peter C. Burns*[b]

Received 12th April 2012
DOI: 10.1039/c2cs35136f

While the d^0 transition-metal POMs of Group V (V^{5+}, Nb^{5+}, Ta^{5+}) and Group VI (Mo^{6+}, W^{6+}) have been known for more than a century, the actinyl peroxide POMs, specifically those built of uranyl triperoxide or uranyl dihydroxidediperoxide polyhedra, were only realized within the last decade. While virtually every metal on the Periodic Table can form discrete clusters of some type, the actinyls are the only—in addition to the transition-metal POMs– whose chemistry is dictated by the prevalence of the '*yl*' oxygen ligand. Thus this emerging structural, solution, and computational chemistry of actinide POMs warrants comparison to the mature chemistry of transition-metal POMs. This assessment between the transition-metal POMs and actinyl POMs (uranyl peroxide POMs, specifically) has provided much insight to the similarities and differences between these two chemistries. We further break down the comparison between the alkaline POMs of Nb and Ta; and the acidic POMs of V, Mo and W. This more indepth literature review and discussion reveals that while an initial evaluation suggests the actinyl POMs are more akin to the alkaline transition-metal POMs, they actually share characteristics unique to the acidic POMs as well. This tutorial review is meant to provide fodder for deriving new POM chemistries of both the familiar transition-metals and the emerging actinides, as well as fostering communication and collaboration between the two scientific communities.

[a] *Sandia National Laboratories, Albuquerque, NM 87185, USA. E-mail: mdnyman@sandia.gov*
[b] *Department of Civil Engineering and Geological Sciences, Department of Chemistry and Biochemistry, University of Notre Dame, Notre Dame, IN 46556, USA. E-mail: pburns@nd.edu*
† Part of a themed issue covering the latest developments in polyoxometalate science.
‡ Current address: Chemistry Department, Oregon State University, Gilbert Hall, Corvallis, Oregon 97331, USA.

Introduction

Polyoxometalate (POM) chemistry is traditionally described as discrete anionic clusters of the early d^0 transition metals, Group V and Group VI; V^{5+}, Nb^{5+}, Ta^{5+}, Mo^{6+}, and W^{6+}. When considering only the solid-state structures that are common to all of these POM-forming metals, one might assume that their aqueous chemistries are similar. In fact,

May Nyman

May Nyman's education is diverse: she received a BSc in Geology, a MSc in Materials Science and Engineering (both from Virginia Tech), and a PhD in Inorganic Chemistry (University of New Mexico). She has worked for Sandia National Laboratories in Albuquerque, NM (USA) since 1998, developing functional materials for environmental and energy applications. These include water-treatment coagulants, sorbents for contaminants and nuclear waste treatment, photocatalysts, ion conductors, and phosphors. Aqueous synthesis of polyionic clusters is May's passion, particularly clusters in aqueous alkaline solutions.

Peter C. Burns

Peter C. Burns received his BS, MS and PhD degrees from the University of New Brunswick, University of Western Ontario, and University of Manitoba, respectively, all in Canada. Following post-doctoral appointments at the University of Cambridge and the University of New Mexico, and one year on the faculty at the University of Illinois, he joined the faculty of the University of Notre Dame in Indiana, USA, in 1997. He is currently Massman Professor of Civil Engineering and Geological Sciences and Concurrent Professor of Chemistry and Biochemistry.

the routes by which these POM clusters self-assemble in water vary significantly between V^{5+}, Mo^{6+}, and W^{6+} *vs.* Nb^{5+} and Ta^{5+}. Oxoanions of V^{5+}, Mo^{6+}, and W^{6+} are monomers in alkaline conditions, and assemble into polynuclear clusters in acidic conditions. On the other hand, there are no known comparable oxoanions of Nb^{5+} and Ta^{5+}, and they form polynuclear clusters in alkaline conditions. Colloquially-speaking and also borrowing from the radioisotope separations literature, we refer to the two types of POMs, based on their aqueous chemistries, as the acid-side (V, Mo, and W) and the alkaline-side (Nb and Ta). What enables the self-assembly of these discrete, water-soluble polyanions is the prevalence of the double-bonded oxygen ligand, known as an *yl* oxygen. The M=O unit is known as a vanadyl, niobyl, *etc*.

Some of the actinides, specifically those in the pentavalent or hexavalent oxidation states, also possess the *yl* ligand, but the actinides have two *trans yl* ligands, and the formal bond order is three; *i.e.* O≡U≡O. The coordination chemistry of U^{6+} is the most developed of the actinides, and the vast majority of complexes and solids exhibit the $(UO_2)^{2+}$ uranyl ion. The recent discovery[1] of actinyl-based POMs has shown that the actinide *yl* oxygen is a necessary (but not sufficient) component of this newest class of polyoxometalate clusters. In the chemical literature, the term polyoxometalates or polyoxometalate-like has been used loosely to include transition metal clusters (*i.e.* of iron or manganese) that do not contain the *yl* oxygen, but are instead surface-passivated by organic ligands. Here we limit and focus on the definition to polyoxometalates as only those that are surface-passivated by the *yl* oxygen and do not contain organic ligands. More than 35 uranyl POMs have been reported, and in each; bidentate peroxo bridges between uranyl ions are essential features. Most of the clusters built only from uranyl ions also have uranyl bridges that are two hydroxyl groups. Clusters containing these two types of bridges form in solution with pH ranging from about 7 to 13. Incorporation of other bridges, including oxalate and pyrophosphate, extends the pH range of cluster formation into acid conditions, as low as pH = 4.

However, based predominantly on the alkaline aqueous conditions required for assembly of the POMs built from uranyl ions with peroxo and hydroxyl bridges, we consider these newest members of the POM family to reside on the alkaline-side. In this tutorial review, we examine the details of this comparison, and discuss POM characteristics and behaviors that are directly related to the aqueous pH range in which they are synthesized and stable. These topics include synthesis, charge and charge density, solubility, acid–base behavior, incorporation of heteroatoms or addenda metals, and the oxides related to the alkaline transition metal and actinyl POMs. Additionally, we will compare more broadly the synthesis, structural features, and properties of the actinyl POMs to the transition-metal POMs on the acid-side. This is the first comparative review of this sort since the inception of the actinyl POMs, and our hope is that it will facilitate and inspire new science in both the familiar landscape of transition-metal POMs and the new frontiers of the f-element POMs.

Role of the *yl* oxygen in cluster formation

Clusters in general represent the size regime between monomers and infinite solids, and they can be stabilized at this intermediate state by either ligands or the *yl* oxygen. Another intermediate-sized entity is nanoclusters or quantum dots, which are passivated also by ligands, more specifically known as capping groups, but ligated clusters or nanoclusters are beyond the scope of this review. Below we discuss briefly how the *yl* oxygen allows isolation of discrete anionic clusters, which is the common link between the transition-metal and actinide POMs. Most aqueous metal cations on the Periodic Table are acidic. This means dissolution of salts of these metals in their stable oxidation states in neutral water results in (1) bonding of water to the metals (hydration); and (2) deprotonation of the bound waters and a resultant decrease in pH. If base is added to these solutions, the hydrated metal cations undergo condensation; or oligomerization *via* formation of M–O–M (M = metal, O = oxygen) bonds. For most metals, this occurs rapidly and without control, and the end result is precipitation of a metal oxide (often hydrous metal oxide). Metals that possess the *yl* oxygen, or a multiply-bonded oxygen ligand behave differently. The reader is referred to Fig. 1 for illustrations of the building blocks of POMs.

The *yl* oxygen is common to d^0 closed shell transition metals of the Group V and Group VI; V^{5+}, Nb^{5+}, Ta^{5+}, Mo^{6+} and W^{6+}: distortion resulting from the second-order Jahn–Teller effect of these metal cations.[2] Trans to the *yl* oxygen is a long metal–oxygen bond: the $M{=}O_{yl}$ bond length is around 1.6–1.8 Å, and the *trans* M–O bond around 2.2–2.4 Å. Some V, Mo and W POMs feature polyhedra with two *yl* oxygens, always in a *cis*-arrangement; some common examples of Mo and W include heptamolybdate and paratungstate, respectively. Vanadates include the mineral sherwoodite featuring isolated $[AlV^{V}_{12}V^{IV}_{2}O_{40}]$ polyanions,[3] and $[NiV_{13}O_{38}]^{18-}$.[4] Monomeric vanadyl is also assumed to coordinate as *cis*-$VO_2(H_2O)_4^{+}$ in water,

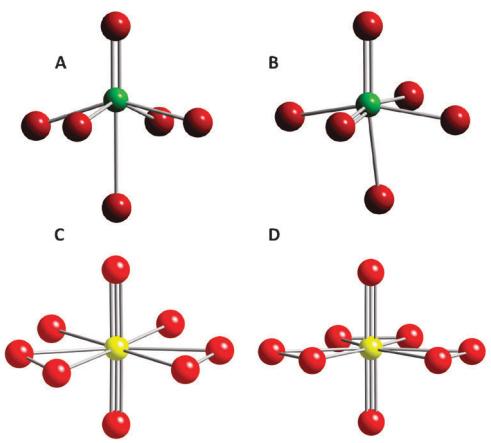

Fig. 1 Monomer building-blocks of transition-metal and actinide POM chemistry. **A** & **B**. green spheres are d^0 Group V and Group VI transition metals V, Nb, Ta, Mo, W. **A** shows a distorted octahedron with a single *yl*-oxygen *trans* to a long M–O bond. **B** shows a distorted octahedron with two *cis*-*yl*-oxygen ligands. **C** & **D** show the uranyl building blocks; yellow spheres are U^{6+}. **C** is uranyl *cis*-dihydroxidediperoxide and **D** is uranyl triperoxide.

based on structures of this isolated monomer.[5] Of course lacunary clusters also have *cis*-yl oxygen ligands as isolated entities, but these provide bonding sites for addenda metals (details below).

The actinyls always carry two *yl* oxygens, but in a *trans* arrangement, and these actinyls include U(VI)O_2, U(V)O_2, Np(V)O_2, Np(VI)O_2, Pu(V)O_2 and Pu(VI)O_2. Actinyl ions arise because of the interaction of atomic orbitals on the actinide and O atoms. Specifically, in the case of the U(VI)O_2^{2+} actinyl ion, there are 12 p electrons from the O atoms that completely fill the bonding orbitals, consistent with the very strong triple bonds that occur in the uranyl ion. There are six linear combinations of oxygen p orbitals in the uranyl ion, some of which have symmetry that only matches with uranium f-orbitals. The importance of f-orbitals in the case of uranyl favors the linear dioxo cation, rather than the bent configuration that occurs in the f-orbital lacking transition metal cases.[6]

The *yl*-oxygen ligands do not readily protonate or bridge to other metal centers. In this sense, as the M–O–M bonded network grows by hydrolysis and condensation reactions, the *yl*-oxygen 'passivates' the growing metal oxide surface so the growth process may stop at a discrete, water soluble size; the exact size controlled by solution variables that will be discussed later. This *yl*-oxygen at the cluster surface provides aqueous solubility without introducing any organic ligands, and POM clusters are very stable in aqueous solution if the pH is appropriate. In this regard, the POMs resemble small and absolutely discrete pieces of soluble metal oxide, which renders them very useful for experimental and computational studies in modeling the solid-aqueous interface: this is one of the many creative uses of POMs. Since the UO_2 unit of the uranyl clusters has the passivating *yl*-oxygen pointing in two directions, it actually forms more shell-like or hollow clusters, and this is discussed later in this review, with regard to the strong templating effect of the alkali cations inside the cluster.

Synthesis of POMs from the acidic and alkaline sides

The acid-side

The aqueous assembly of POM clusters is quite different for POMs of V^{5+}, Mo^{6+} and W^{6+} *vs.* Nb^{5+} or Ta^{5+}. The actinyl POMs have components resembling each general synthetic route. By far the most developed actinyl POMs are the uranyl POMs featuring U(VI)O_2, and these will be discussed in most detail throughout this review. For the acid-side POMs of V^{5+}, Mo^{6+} and W^{6+}, the synthesis starts with the very water soluble alkali salts of the oxoanion monomer, VO_4^{3-}, MoO_4^{2-} and WO_4^{2-}. When these are dissolved in water, the pH goes up, generally above 12, *via* protonation of the oxo-ligands of the oxoanion. The oxoanions simultaneously expand their coordination sphere by binding water. Subsequent addition of acid results in hydrolysis and condensation reactions, checked by the predominant *yl*-oxygen, and the final result is soluble, discrete anionic POM clusters. The size, geometry and monodispersity of the POM clusters that form is dependent on many factors including pH, concentration of the POM-forming metal, presence of heteroatoms or addenda metals,

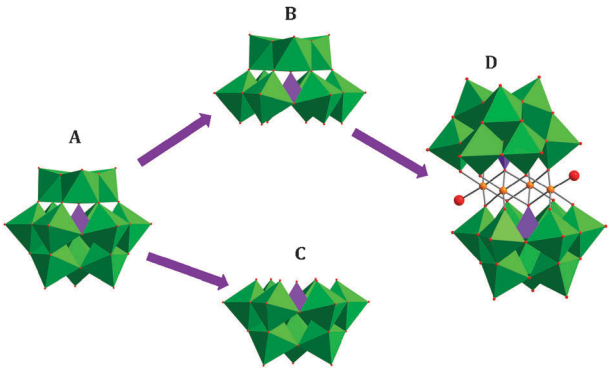

Fig. 2 Illustrating plenary, lacunary, heteroatom and addenda metal in transition-metal POM chemistry. (**A**) Plenary α-Keggin ion, $[XM_{12}O_{40}]$. Green octahedra are POM-forming metals M = Nb, Mo, or W. Purple tetrahedron is the heteroatom in POM chemistry; *i.e.* Si, Ge, Al, P. (**B**) A-type trivacant Keggin ion, $[XM_9O_{34}]$ derived by removing three corner-sharing octahedra from the plenary Keggin ion. (**C**) B-type trivacant Keggin ion, $[XM_9O_{34}]$ derived by removing three edge-sharing octahedra from the plenary Keggin ion. D) Two B-type trivacant Keggin ions sandwiching three open-shell transition metal octahedra (*i.e.* Co^{II})—these are the addenda metals in POM chemistry (Co = orange spheres, aqua ligands = red spheres).

and counter-cations. For the non-specialist, it is important to distinguish heteroatoms and addenda metals at this point, in the realm of transition-metal POM chemistry. Heteroatoms are an integral part of the cluster, the central tetrahedral metal (P^{5+}, Si^{4+}, *etc.*) for instance of the common Keggin ion and its many derivatives. Addenda metals link complete clusters (plenary) or cluster fragments (lacunary) together to form larger cluster units. An example is the sandwich POMs, where the 'bread' is lacunary phospho (or silico) tungstates and the 'filling' is transition-metal polyhedra (iron, manganese, cobalt, *etc.*)[7] Fig. 2 shows the plenary α-Keggin ion, lacunary derivatives and a sandwich compound, illustrating the concepts of plenary, lacunary, heteroatom and addenda metal.

The alkaline-side

The POM clusters of Nb^{5+} and Ta^{5+} assemble by a different aqueous route. There are no oxoanions, NbO_4^{3-} or TaO_4^{3-}; perhaps due to their larger radius and relative aqueous instability of the tetrahedral coordination. Niobium and tantalum oxides are amongst the few transition metal oxides that dissolve in aqueous base and precipitate in aqueous acid. To form a POM of Nb^{5+} or Ta^{5+}, Nb_2O_5 or Ta_2O_5 can either be (1) dissolved in a strongly alkaline solution, or (2) fused with an alkali hydroxide and then dissolved. Both routes lead to the same endpoint—formation of the Lindqvist POM cluster, $[M_6O_{19}]^{8-}$; M═Nb,Ta, one of the most common plenary POM geometries. (Fig. 3) For the acidic POMs; in general, plenary clusters are assembled at the lowest pH values, and the lacunary clusters are derived from these usually by increasing the pH so that M═O units are 'plucked' out of the cluster in a controlled fashion. The extreme end of this process is disassembly of the POM clusters to their monomer (or small oligomer) precursors. One might expect the corollary from the alkaline side is a decrease of pH from that which stabilizes the Lindqvist cluster could result in related lacunary clusters.

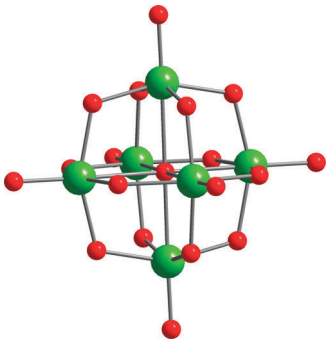

Fig. 3 The Lindqvist ion—the most common POM geometry for alkaline transition metal POMs: $[M_6O_{19}]^{8-}$ M = Nb,Ta. Green sphere is Nb,Ta; red sphere is oxygen.

However, this is not the case in ambient conditions: decrease in pH just results in precipitation of the oxide. This is the key difference between the acid POM metals that have the stable monomer form, and the alkaline POM metals for which there is not a stable aqueous monomer. In order to obtain other Nb-POM geometries, the Keggin ion derivatives in particular, hydrothermal processing is required, in slightly less alkaline conditions (pH ~10.5–13) than that which the Lindqvist ion forms with ambient processing (in an open beaker, heating only up to approximately 90 °C). The combination of the slightly lower alkalinity and heat allows retention of solubility of POM fragments and partial destruction of the Lindqvist ion so other cluster geometries can assemble. Recent developments in polyoxoniobate chemistry have been reviewed in detail in 2011,[8] and we refer the readers to this article for more details, as this is not the main point of the current review.

The uranyl POM clusters self-assemble quite readily in alkaline solutions in the presence of peroxide in ambient conditions. Where the monomer building block of the transition metal POMs is most commonly MO_6 and less commonly MO_4 and MO_5 (M = V, Nb, Ta, Mo, W), the most frequently observed monomer building blocks (see Fig. 1) for the uranyl clusters is uranyl triperoxide, $UO_2(O_2)_3^{4-}$ and uranyl diperoxidedihydroxide, $UO_2(O_2)_2(OH)_2^{4-}$, with the hydroxyl ligands in *cis* orientation. Thus far, the peroxide ligand seems necessary to provide curvature for cluster formation. The U–peroxide–U interaction is inherently bent, due to the combinations of electronic orbitals, and these details are discussed elsewhere.[9,10] DFT simulations indicate that the dihedral angle of the U–(O_2)–U bridge is ideally ~140°, and this is consistent with the geometries of reported cage clusters in general.[9,11] If all uranyl ions in a cage cluster are bridged only through peroxide groups, the size of the cluster is limited by the dihedral angle of the bridge, because of the curvature required. Incorporation of hydroxyl bridges between uranyl ions generally fosters formation of larger clusters, such as U_{50} and U_{60},[10] because the dihedral angles for U–$(OH)_2$–U bridges are flatter, as shown by the DFT simulations. It is the average dihedral angle for the aggregate of bridges between uranyl ions in a cage cluster that is most important in determining its size. In turn, accurate reproduction *via* computation of the experimentally determined U–(O_2)–U or U–$(OH)_2$–U angles in capsules depends heavily on inclusion of the templating alkali countercation in the model for computation. Thus the energetics of the dihedral angles that define capsule geometries can be most accurately calculated when considering the alkalis.

From the point of view of synthesis, the uranyl peroxides are similar to the alkaline POMs, in that they self-assemble in aqueous base, and precipitate a chemically related oxide-peroxide phase in lower pH (studtite for instance, $[(UO_2)O_2(H_2O)_2]\cdot 2(H_2O)$[12]). However, the ability to isolate stable $UO_2(O_2)_3^{4-}$ and $UO_2(O_2)_2(OH)_2^{4-}$ monomers as alkali salts of Li, Na or K[13–16] is more akin to the acid POM chemistry—in that stable alkali salts of VO_4^{3-}, MoO_4^{2-} and WO_4^{2-} are isolatable forms and are commonly used to synthesize POM clusters. In fact, the alkali salts of the $UO_2(O_2)_3^{4-}$ monomer can be used as precursors for the uranyl peroxide clusters.[15] The $UO_2(O_2)_2(OH)_2^{4-}$ monomer, on the other hand, has been isolated only with the OH ligands in the *trans*-position,[17] whereas they have a *cis*-orientation in all the uranyl clusters containing this monomer building block. Nb and Ta also form water-soluble peroxide-ligated monomers; $Nb(O_2)_4^{3-}$ and $Ta(O_2)_4^{3-}$ that are readily precipitated as NH_4^+, K^+, Rb^+ and Cs^+ salts.[18] These, in fact, have been used to synthesize the $[Ta_6O_{19}]^{8-}$ Lindqvist ion.[19] The difference between the synthesis of the Ta-POMs and the U-POMs from the peroxide monomer precursors is the U-POMs appear to need to retain the peroxide ligands to provide curvature necessary for cluster formation, whereas the peroxide ligand is replaced by oxo ligands in the Ta-POMs. There are some examples of Nb-POMs that contain peroxide ligands, and these will be discussed later.

The role of internal countercations

Unlike the other topics discussed in this review, the focus of alkali templating of clusters is actually better developed for the actinide POMs than for the transition metal POMs, which arises from the unique capsule-like nature of these clusters. Since the *yl*-oxygens of the uranyl passivates the internal curved surface of the cluster as well as the external surface, the result is shell-like clusters that encapsulate water and alkali cations. The $UO_2(O_2)_3^{4-}$ or $UO_2(O_2)_2(OH)_2^{4-}$ building blocks are linked into square, pentagonal and hexagonal rings by polyhedral edge-sharing of the peroxide ligand, or the two *cis*-hydroxyl ligands. In these rings that are concave toward the center of the capsule, the *yl* oxygen atoms point toward the center on the concave side, creating a perfect inorganic crown for binding a metal. It has been observed both synthetically and computationally that the size of the ring is selective toward the size of the alkali, with squares hosting Li, pentagons hosting Na and K,[20,21] and hexagons hosting Rb and Cs, and sometimes K.[1,15,22] (see Fig. 4) The K-templated pentagonal ring is the only uranyl peroxide ring that has been isolated (with oxalate ligands, $K_{10}[(UO_2)(O_2)(C_2O_4)]_5$) and structurally characterized,[21] the rest have been observed in fully-formed capsules only. Li in a square ring has only been observable crystallographically templating the squares of the Np_{24} cluster, $[Li_6(H_2O)_8NpO_2(H_2O)_4\{(NpO_2)(O_2)(OH)\}_{24}]^{20-}$.[1] We assume they are likewise located on the inside of isostructural U_{24} because (1) Li is the only alkali present in the reaction solution, and (2) it is not likely that these capsules are empty.

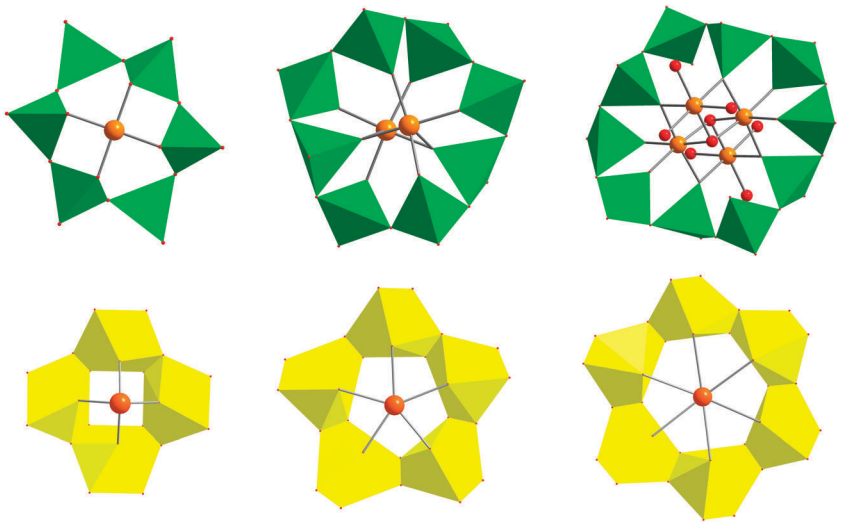

Fig. 4 Templated ring structures in transition-metal and actinyl POM chemistry. Top row is isolated VO_4 rings templated with transition metals (green polyhedra are VO_4, orange spheres are transition metals and red spheres are aqua ligands): $[PdV_6O_{18}]^{4-}$ (left), $[Cu_2V_8O_{24}]^{4-}$ (center) and $[Ni_4V_{10}O_{30}(OH)_2(H_2O)_6]^{4-}$ (right).[29] Bottom row is square, pentagonal and hexagonal rings templated by alkalis within actinyl POM capsules; view is from inside the capsule (yellow polyhedra are actinyls, orange spheres are alkalis): Li templating a square ring in the Np_{24} cluster (left);[1] Na or K templating a pentagonal ring in U_{28}, for instance (center); Rb or Cs templating a hexagonal ring, also in U_{28}.[15,33]

We also make the assumption that these Li-cations have some degree of disorder, which renders them more difficult to locate. The A^+–*yl*–O bond lengths within these cavities are typical of the alkalis: Li–O ~1.8–2.2 Å, Na–O ~2.3–2.7 Å, K–O ~2.6–3.0 Å, Rb–O ~2.9–3.2 Å, and Cs–O ~3.0–3.6 Å. These bond lengths add slightly more than 10% of the BVS value of the *yl*-oxygen per bonded alkali, which obtains most of its bond valency from multiple bonding to U^{6+}. Furthermore, the U–O_{yl} bond length does not correlate with number of bonded alkalis, where 0–3 bonded alkalis have been observed over numerous structures. What is not entirely clear though, is the role of the alkalis in the growth of the clusters. They may actively template growth of rings and then capsules, or they may simply stabilize highly anionic cluster fragments by binding in appropriately-sized multidentate cavities. However, in the absence of the appropriate experimental studies in solution, this discussion is simply speculation for the moment, and represents a considerable area for growth of this science. Aqueous phase studies of the cluster assembly process, such as by light or X-ray scattering, nuclear magnetic resonance studies, or vibrational spectroscopies are experiments that should be undertaken in the future to identify the putative ring-shaped building blocks *in situ*, and their subsequent (or simultaneous) conversion to the capsules that we observe on the solid state.

There are also examples of alkalis templating the rings on the outside of the capsule, or the convex side of the ring. However, these alkalis bond to the peroxide ligands instead of the *yl*-oxygens. For example, in a K/Cs^+ templated U_{28} cluster (U_{28} = $[UO_2(O_2)_{1.5}]_{28}$, an all-peroxide linked uranyl capsule), K^+ is hosted inside the pentagonal rings (K–O_{yl} = 2.6–2.8 Å), while Cs is nested on the outside of the pentagonal ring (Cs–$O_{peroxide}$ = 2.9–3.1 Å). A far more common bonding mode of the alkalis outside the cluster is by side-on bonding of the cluster peroxide bridge to the alkali. Fig. 5 shows alkalis bonded externally to uranyl POM capsules.

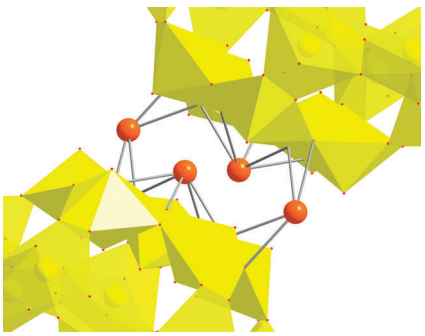

Fig. 5 View showing two modes of bonding of Cs^+ counterions to the outside of U_{28} capsules within its crystalline lattice; orange spheres are Cs and yellow is the uranyl polyhedra.[15] The Cs^+ central to the image sit above the pentagonal rings of two adjacent clusters, and the other two Cs^+ coordinate side-on to bridging peroxide ligands of the clusters. This view also illustrates how these large alkali bridge the clusters to create an poorly soluble lattice network of cations and anions.

There are no examples of POMs of Ta or Nb in which the charge-balancing alkali cations reside within and template the cluster internally. On the other hand, there are some examples of V, Mo or W-POMs where a single alkali appears to play a templating role, and these have generally been termed cryptands. Many of these are actually two lacunary fragments that sandwich a cation of a specific size or charge.[23–26] From the acid-side, square and pentagonal rings of corner-sharing VO_4 tetrahedra are documented in aqueous solution[5] (and these contain no alkali cations), and the square ring has been isolated in the solid state.[27] Furthermore, the pentagonal ring ($[Mn_2V_{10}O_{30}]^{6-}$ and $[Co_2(H_2O)_2V_{10}O_{30}]$),[28] a hexagonal ring ($[PdV_6O_{18}]^{4-}$), an octagonal ring ($[Cu_2V_8O_{24}]^{4-}$),[29] and a decagonal ring ($[Ni_4V_{10}O_{30}(OH)_2(H_2O)_6]^{4-}$)[29] have been isolated, hosting transition metals within their cavities. Some representative examples are shown in Fig. 4, compared to the templated

uranyl peroxide rings. Similar chemistry with the uranyl POMs would be an area for opportunity and extreme interest. However, the alkaline conditions usually required to form these presents a challenge (discussed later).

The family of giant molybdate POMs that were first reported by Achim Muller in the mid 1990's,[30] like the uranyl-POMs, also incorporate alkali metals and water. These self-assemble over several weeks in a sodium molybdate solution to which an acidic reducing agent (ascorbic acid, for instance) is added. The giant 'blue' clusters (indicating reduced Mo^{V} and/or Mo^{IV} centers or delocalized electrons are present) are capsule-like, contain hundreds of metal polyhedra in the transition metal shell (also have been formed with mixed Mo/Fe and Mo/V), and do indeed encapsulate anions, cations, and water. These encapsulated species however do not appear to play any templating role on the cluster growth: they are disordered and not bound tightly to the internal curved surface of the molybdate shell. However, extensive and detailed ion exchange studies have been carried out with these capsules.[31,32] These studies have revealed that both cations and anions can exchange into the capsules, the exchanged-in ions can bond to the internal curved surface of the capsule, and the pores through which the ions are transported are flexible in the aqueous environment and can open and close in response to the composition of the aqueous medium.

Comparatively, the dynamic behavior of the alkali cations encapsulated within the uranyl POM capsules has been only discussed briefly; but this phenomenon has enormous potential for future detailed studies. Nyman *et al.*[15] initially noted that U_{28} with K and Cs templating the pentagonal and hexagonal rings respectively (and $Ta(O_2)_4$ residing in the center of the capsule) will rapidly exchange all of the internal K^+ for Na^+ in a solution of excess Na^+. In a subsequent publication, a crystal structure of the Na-exchanged U_{28} was reported, and computational studies revealed the stabilization energy of the Na-analogue relative to the K-analogue.[33] It was also shown that the Cs^+ could slowly exit the capsule, depending on the nature of the central templating anion. The peroxometalates, $Nb(O_2)_4^{3-}$ or $Ta(O_2)_4^{3-}$ located in the center of the capsule appear to provide better stabilization towards retaining the encapsulated alkali cations than the central uranyl anion.[15] Perhaps this is because the peroxometalates bind the internal alkali cations more tightly. The prior work of Muller *et al.*, revealing the flexibility of the porous openings in the capsule shell is most certainly expected here as well, given the fact that the Cs^+ cation is large yet is able to exit the cluster. Ion-exchange also presents an underutilized method to develop new forms of these uranyl POMs. Dynamics, structure and energetics of uranyl POMs as a function of alkali countercations will definitely play a significant role in the future development and understanding of this POM family.

Another POM phenomenon involving alkali countercations is the assembly of the macrostructures in solution dubbed 'blackberry structures', pioneered by Tianbo Liu.[34] In these assemblies, clusters associate as a closest-packed array, forming the surface of a hollow sphere, and alkali countercations bridge these clusters through anion-cation-anion association. Weinstock[35] further observed similar arrays forming on the surface of gold nanoparticles, with the anionic POMs replacing citrate anions.[35] The blackberry structures have thus far been only observed for larger POM clusters with low charge density. In fact, the blackberry formation is often initiated by alkali cation-POM association, induced by addition of a less polar solvent to the aqueous POM solution: smaller POMs with higher charge such as Nb-POMs may actually simply precipitate under such solution conditions. On the other hand, cation-mediated assembly of POMs on the gold nanoparticle surface was observed for the small and highly-charged lacunary Keggin ion, $[AlW_{11}O_{39}]^{9-}$.[35] Therefore, 'blackberry formation' from smaller POM clusters of higher charge, a category which includes both the alkaline POMs and the uranyl POMs, may be an effort for future development of alkali-mediated POM assembly on both surfaces and in solution.

Charge-density of POMs

Table 1 (adapted from Nyman[8]) summarizes the charge-densities of some common Nb and W POM clusters, along with a few uranyl POMs. Here we can clearly see that the Group V POMs possess higher charge-density than Group VI POMs, as expected; and this scales with pH of synthesis. Generally higher charged clusters assemble and are stable at higher pH. The lacunary Group VI POMs, such as $[PW_9O_{34}]^{9-}$ are also formed at higher pH (*i.e.* $\sim$8). While this is straightforward for the transition-metal POMs, the comparable analysis of the uranyl POMs is complicated by the encapsulated cations, anions and water molecules. Firstly, for many of the uranyl POMs, the encapsulated species are not well-defined, due to disorder. We identified three well-described uranyl POMs and included these in Table 1, both with and without their encapsulated species. Including the encapsulated species gave charge-densities more akin to the polytungstates, while the uranyl shells alone (without considering the encapsulated species) gave charge-densities similar to the polyniobates. Again, the nature of these encapsulated species, their dynamics, structure directing capabilities, and their role in stabilizing the capsules will become clearer with experimental and computational studies focused on these aspects.

The role of external countercations

In the synthesis, crystallization, dissolution, phase transfer and selective precipitation of POMs, the countercations are of utmost importance, and these can include ammonium or phosphonium cations as well as the most commonly-used alkalis. Generally speaking, larger organic cations such as the NR_4^+ (R = alkyl or aryl) series are useful for stabilizing larger clusters with low charge density, as they likewise possess low charge density. These cations also function in the transfer of POM clusters into nonaqueous solvents. This is done quite readily for POMs of molybdate, tungstate and vanadate. As a result, nonaqueous chemistry and applications can be carried out on POM clusters including catalysis, electrochemistry, and functionalization of POMs with organometallic species.[36,37] Nb-POMs, on the other hand, do not readily transfer into non-aqueous solutions, probably due to their high charge-density and close physical association with alkali cations.[38]

Table 1 Charge-densities of POM clusters: Nb-POM (blue), W-POM (orange), U-POM with Encapsulated Species (yellow) and U-POM without Encapsulated Species (gray)

Formula	Charge (-)	# atoms (non-H)	Charge density (charge/#atoms)
$[Nb_6O_{19}]$	8	25	0.32
$[SiNb_{12}O_{40}]$	16	53	0.30
$[(PO_2)_3PNb_9O_{34}]$	15	53	0.28
$[(UO_2)_{16}(O_2)_{24}(OH)_8]$ [22]	24	104	0.23
$[Ti_2Nb_8O_{28}]$	8	38	0.21
$[GaNb_{18}O_{54}]$	15	73	0.21
$[PW_9O_{34}]$	9	44	0.20
$[(UO_2)_{20}(O_2)_{24}(P_2O_7)_6]$ [55]	32	162	0.20
$[H_2Si_4Nb_{16}O_{56}]$	14	76	0.18
$[\{(UO_2)(O_2)_{1.5}\}_{28}]$ [15]	28	168	0.17
$[Nb_{10}O_{28}]$	6	38	0.16
$[SiW_{11}O_{39}]$	8	51	0.16
$[K_8(UO_2)_{20}(O_2)_{24}(P_2O_7)_6]$ [55]	24	170	0.14
$UO_4Na_4Cs_4(H_2O)_9[(UO_2)_{16}(O_2)_{24}(OH)_8]$ [22]	14	126	0.111
$[W_6O_{19}]$	2	25	0.080
$[Rb_4K_{12}[Nb(O_2)_4]\{(UO_2)(O_2)_{1.5}\}_{28}]$ [15]	15	193	0.078
$[SiW_{12}O_{40}]$	4	53	0.075
$[P_2W_{18}O_{62}]$	6	82	0.073

Therefore nonaqueous POM chemistry of the alkaline niobates and tantalates is virtually nonexistent; again due to the high charge-density of these clusters. However, there are a few exceptions. Decaniobate, $[Nb_{10}O_{28}]^{6-}$, for instance, is synthesized in ethanol with tetramethylammonium (TMA) counterions.[39] It has the lowest charge-density of Nb-POM clusters (see Table 1), and converts to $[Nb_6O_{19}]^{8-}$ in more alkaline solution. The decaniobate can also be reversibly dimerized, and this too takes place in nonaqueous solvent, with tetrabutylammonium (TBAOH) counterions.[40] Additionally, a diprotonated hexatantalate $[H_2Ta_6O_{19}]^{6-}$, also with TBAOH countercations was crystallized from a toluene-ether mixture.[41] This non-aqueous hexatantalate example may be an isolated incident, or it may point towards the future of Ta-POM chemistry, which has thus far eluded significant development.

Nonaqueous uranyl POM chemistry has not yet been explored, and represents opportunity for researchers. According to Table 1, the charge-density of a typical uranyl POM cluster with their encapsulated species is more similar to that of the acidic POMs than most of the highly charged alkaline POMs, which suggests nonaqueous chemistry of the uranyl POMs may be readily achievable. The potential benefits of this putative non-aqueous uranyl POM chemistry include opportunity to investigate redox chemistry of the clusters more indepth, and stabilization of the dynamic alkali's, by removing the uranyl POM from its aqueous environment.

Another chief function of countercations in POM chemistry is to serve in the dissolution or precipitation of clusters, for the purpose of aqueous phase studies, and crystallization/purification, respectively. The usual trend with alkali POMs is, the smaller alkalis (Li, Na) are useful for dissolution, while the larger alkalis (Rb, Cs) help in rapid precipitation of pure phase clusters, when a single cluster geometry dominates in solution. Meanwhile, K can go either way, and is always a good starting point when one is interested in dissolving or precipitating POMs. This usual trend is what we have come to expect based on hydration behavior of these cations. Smaller cations tend to be solvent-separated from their anions with large hydration spheres, while larger cations are more prone to contact ion-association. The larger alkalis not only associate to a single anion (such as a POM) in aqueous solution, but they bridge between the anions, which ultimately results in rapid aggregation and precipitation.

This common trend that is observed for the POMs of V, Mo and W is in fact what is observed for the uranyl POMs—not only for the clusters, but the monomer forms as well. For instance, the Cs salts of U_{28} reported prior[15] are insoluble in neat water, and the Rb salts are only sparingly soluble.

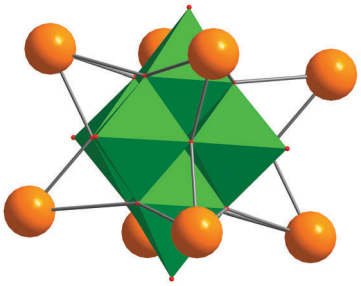

Fig. 6 The $[M_6O_{19}]^{8-}$ Lindqvist ion (M = Nb, Ta) with eight associated Cs^+ cations. This mode of bonding to the face of the superoctahedron Lindqvist ion is also common to coordination complexes with transition metals.

(Fig. 5 shows U_{28}, emphasizing external associated Cs-cations) However, these clusters can be redissolved with the addition of a Li, Na, K, or TMA electrolyte solution. The cautionary note, however, in utilizing large alkalis such as Cs for precipitating uranyl POMs is the solutions of self-assembling clusters are not always monospecific. Thus if the precipitation is not carried out in a controlled manner or with optimal timing, a mixture of products whose identity is not readily determined can result.

The POMs of Nb exhibit a very unusual solubility trend with their alkali countercations, and this trend is opposite that of the uranyl POMs and the POMs of Mo, V and W. This was first noted for the common $[Nb_6O_{19}]$ Lindqvist ion, in that the Li and Na salts were sparingly soluble,[19,42] while the Rb and Cs salts were extremely soluble.[8,43] However, what is more fascinating is that while the solubility trend is anomalous, the alkali-POM bonding is classic in the solid-state, with a neutralized complex forming with Rb and Cs where each face of the octavalent superoctahedral cluster tightly binds an alkali, $A_8[Nb_6O_{19}]$. (Fig. 6) Furthermore, the direct bonding of the heavy alkalis to $[Nb_6O_{19}]^{8-}$ persists in solution.[38] The initial Keggin-ion heteropolyniobate derivatives with Na^+ or Li^+ were also found to be relatively insoluble.[42,44,45] However, it was not until very recently that the Nb-Keggin derivatives with Rb and Cs countercations have been isolated;[46] and these salts are extremely soluble, confirming the universality of the anomalous solubility trend of Nb-POMs. This anomalous solubility trend of the Nb-POMs is not well-understood. However, it presents an ideal opportunity to understand the relationship between cation-anion pairing in solution, charge-density, acid–base behavior and solubility of ionic clusters (and more generally any salts) in water. There is not yet enough known about aqueous behavior of the related Ta-POMs, $[Ta_6O_{19}]^{6-}$ in particular,[19,47] to determine if these follow the same anomalous solubility trend as a function of alkali countercation size. This too represents a ripe area for future exploration.

Protonation of POM clusters

Protonation of POM cluster oxygen ligands warrants some discussion here, as it plays an important role in cluster growth and aqueous dynamics of clusters and their monomer precursors, for both the transition metals and actinides. In crystalline lattices of POM clusters, protonated oxygen ligands, or hydroxyl ligands can be observed directly or inferred, often through bond-valence calculations. In almost all cases where the proton is observed directly, it resides on bridging μ_2 or μ_3 oxygen positions, rather than the terminal = O_{yl} site, illustrating the relative lack of reactivity of this ligand, or its lower basicity. In a classic paper by Klemperer—*Where are the protons*?[48]—the locations of protons on decavanadate are inferred, based on proton NMR in solution and the dimer-arrangement of the clusters in the solid-state, presumably associated by H-bonding of the bridging μ_2–OH–V_2 ligands to the adjacent cluster. Protonation of alkaline POMs is common and expected, based on their high charge-density. Mono-, di- or even tri- protonation of the hexaniobate Lindqvist cluster, $[H_xNb_6O_{19}]^{8-x}$ (x = 0–3) with the highest charge-density of all POM clusters is observed directly *via* crystallography in many structures,[43,49,50] or inferred by charge-balance coupled with bond valence sum (BVS) calculations, identifying oxygen ligands within the cluster that are underbonded.[19] Observation of protonation directly is often facilitated by hydrogen bonding to a second cluster or a water molecule, which holds the proton rigid and allows its observation. On the other hand, there are many examples of polyoxoniobates[42,51] (and vanadates, tungstates and molybdates as well[52–54]) in which protonation is inferred by charge-balance (*i.e.* not enough countercations to balance the cluster charge), but cannot be located directly in the X-ray map and also cannot be definitively inferred by BVS. In these cases, the unsatisfactory description of disordered protonation is given. There is one unusual example of protonation of a terminal oxygen in polyniobate chemistry. In this example, the Nb_{24} cluster is composed of three heptaniobate (Nb_7O_{22}) building blocks that are linked by three NbO_6 polyhedra, and a Nb–OH bond is inferred *trans* to the Nb=O_{yl}, by BVS calculations.[51] However, these are also not directly observed in X-ray-generated electron density maps.

Crystallization of uranyl peroxide clusters with protons on bridging oxo ligands occurs as well. However, these are better described as hydroxyl ligands. The distinction from the transition metal POMs is that when oxo ligands are present at the equatorial vertices of uranyl hexagonal bipyramids in the uranyl clusters, all the oxos are protonated (hydroxyls), rather than a subset of the oxo ligands. In fact, U-*O*-U bridging oxo ligands are not a known entity in uranyl peroxide POM chemistry. However, P-*O*-U or W-*O*-U bridging oxos are present in cases where WO_4 or P_2O_7 oxoanions serve as equatorial ligands in uranyl peroxide clusters (which are discussed further, below).[55] Amongst all the uranyl peroxide POM clusters reported to date, only U_{20}, U_{28} and U_{44} have $UO_2(O_2)_3$ polyhedra only. The rest have $UO_2(O_2)_2(OH)_2$ only, or both $UO_2(O_2)_2(OH)_2$ and $UO_2(O_2)_3$[1,10,20] In all of these, the protons of the hydroxyl ligands are not observed directly by X-ray diffraction, as they are likely masked by the very high electron density of the uranium atoms, or perhaps they lack rigidity and directionality in the crystalline lattice. The typical U–OH bond length is ~2.25–2.45,[1] with a BVS of the oxygen of ~1; which definitely indicates a hydroxyl, rather than an oxo. Given the importance of the $UO_2(O_2)_2(OH)_2$ unit in uranyl peroxide clusters, it would be valuable to observe these hydroxyl protons by direct methods: perhaps a single-crystal neutron diffraction study would provide this missing evidence for the structure of this somewhat ubiquitous hydroxyl ligand.

Like the transition metal POMs, not all countercations are always located for the uranyl POMs. In fact, this situation may be exasperated by the presence of very heavy uranium atoms. Specifically, the U(VI) cations scatter X-rays much more efficiently than any other constituent in the structure, and the diffraction pattern mostly reflects the arrangement of U(VI), although the counterions may be in a lower-symmetry distribution. This is especially true when lithium or sodium serve as countercations—lithium is often too 'light' to locate, particularly in the case of water-cation disorder in the lattice. Sodium-water disorder is also commonly inferred; the Na–O bond distance and the O–H–O hydrogen bonding distance are similar, approximately 2.6 Å, and the X-ray scattering factors of Na and H_2O are similar, especially relative to the dominance of U(VI) in scattering. Disordered protonation of uranyl POMs may also be considered when not all countercations are well-defined. The potential location of disordered protons include on the *yl*-oxygens and the aforementioned U-*O*-P or U-*O*-W bridging oxygens. There is both experimental and computational evidence for protonation of *yl* or terminal oxo ligands for the transition-metal POMs, see for instance Ganapthy *et al.*[56]

Protonation and oxo ligand exchange of the alkaline POMs $[H_xNb_6O_{19}]^{(8-x)-}$, $[H_xTa_6O_{19}]^{(8-x)-}$ (x = 0–2),[47,57] and $[H_xNb_{10-y}Ti_yO_{28}]^{(6+y-x)-}$ (x = 0–3, y = 0–2)[39,58] has been studied extensively in solution, and also the decavanadate, $[H_xV_{10}O_{28}]^{(6-x)-}$ (x = 1–3).[59] These studies are facilitated by oxygen-17 labeling for NMR studies. While many POMs have been characterized in solution using the ^{17}O label,[60] it is generally only the alkaline POMs that exhibit extensive protonation and thus protonation-dependent oxo-ligand exchange. Of course all studies are limited to the pH range that each cluster is stable: greater than 9 for hexaniobate and hexatantalate, greater than 7 for $[TiNb_9O_{28}]^{7-}$ and $[Ti_2Nb_8O_{28}]^{8-}$, ~6–7.5 for decaniobate, and ~2–6 for decavanadate. These studies define the pH regions in which deprotonated, monoprotonated and diprotonated clusters dominate, the degree of protonation increasing with decreasing pH. These cumulative studies also reveal that oxo ligand lability increases on both sides of the pH stability range (with the exception of hexaniobate, hexatantalate and $[Ti_2Nb_8O_{28}]$, in that these are stable out to the high end of the pH scale.) This universal behavior was explained by a very recent computational study in which Rustad and Casey[61] suggest the intermediate state of POM oxo ligand exchange is always a 'stuffed POM' with an associated hydroxide (high pH) or H_3O^+ (low pH) overbonding a metal center. The oxo ligand exchange is accelerated at high pH because the addition of hydroxide is sterically easy, and is accelerated at low pH because once the hydronium is inserted, protons rapidly distribute over the most basic oxo ligands. In the studies specifically comparing the behavior of $[H_xNb_6O_{19}]^{(8-x)-}$ and $[H_xTa_6O_{19}]^{(8-x)-}$, Casey found that at pH > 12 where there is no pH dependence of oxo ligand exchange, the bridging μ_2–O ligand exchanged faster than the *yl* oxygen for hexaniobate, but the reverse was true for hexatantalate.[47] This curious result, in conjunction with the slightly longer μ_2–O–Nb bonds than μ_2–O–Ta bonds and slightly longer *yl*–O–Ta bonds than *yl*–O–Nb bonds in numerous isostructural crystalline lattices[19] suggested the $=O_{yl}$ ligand was more basic for the tantalate analogue and the μ_2–O ligand was more basic for the niobate analogue. At the time of Casey's and Nyman's solution and solid-state studies, respectively, there were no solid-state structures of protonated hexatantalate clusters. In absence of this data, it was assumed that the *yl*-oxygen ligands protonated more readily. However, more recently, a diprotonated hexatantalate has been published,[41] and the protons do indeed reside on the bridging μ_2-oxygens. On the other hand, this cluster salt was crystallized from non-aqueous solution, and therefore does not necessarily reflect the aqueous state of the hexatantalate.

Analogous oxygen ligand exchange studies to understand solution behavior of the uranyl POMs are yet to be successfully performed. In related work, Grenthe and Szabo[62] used ^{17}O labeling experiments to study oxo (*yl* and OH) ligand exchange of the UO_2^{2+} monomer in TMAOH (tetramethylammonium hydroxide) solutions, where the $UO_2(OH)_{4-5}$ complex dominates. It was found that the exchange rate of the *yl* oxygen with bulk water was dependent on the concentration of the uranyl species, and thus suggested that formation of some sort of dimer intermediate was necessary for exchange. Oxygen ligand exchange studies on the uranyl POM clusters would be useful as they have been for the transition metal POMs, towards understanding acid–base and dynamic behavior of the clusters in water. These studies would be particularly useful for the clusters containing hydroxyl ligands as well as the ubiquitous *yl* oxygen. However some initial attempts at these studies suggested complex solution behavior that involves rearrangement of the clusters, which may or may not be related to dynamic behavior of the alkali cations inside the clusters. This sort of precise and quantitative study that has been carried out with the Group V POMs of pentavalent V, Nb and Ta requires the cluster geometry to not change while monitoring the ligand exchange process. Thus this represents an opportunity for the future of the still-emerging field of actinide POMs.

Heteroatoms and addenda metals in alkaline POM chemistry

The alkaline conditions (greater than pH-7) required to assemble the POMs of Nb, Ta, and U plague the opportunity to incorporate most metals into the clusters. POM clusters of V, Mo and W include encapsulated, linking, and sandwiched transition metals,[63] rare-earths[64] and even actinides.[65] These metals introduce properties and derived applications including luminescence, catalysis, magnetism, specific metal sequestration and redox character. Furthermore, intricate frameworks and very large clusters can be grown. On the other hand, when these metals are introduced to alkaline POM solutions without protective ligands, they precipitate insoluble metal hydroxides: thus the difficulty in mimicking this rich and enviable chemistry of the acid-side. The most successful addenda-metal chemistry for the alkaline Nb-POMs is the Cu-amine complexes. Copper(II) complexes with amines such as ammonia or ethylenediamine are soluble and stable in base. They tend to form octahedral complexes with four Cu–N equatorial bonds and two Cu–O bonds to the cluster ligands. The copper amine complexes serve as charge-balancing cations, and they link

Nb-POMs, $[Nb_6O_{19}]$ in particular, into chain-like or layered phases.[50,66] Most importantly, they have been instrumental in the isolation of novel Nb-POM cluster geometries including clusters containing the heptaniobate fragment $[Nb_7O_{22}]^{9-}$,[51,67] and $[CuNb_{11}O_{35}H_4]^{9-}$.[68] Recently, this strategy utilizing copper amine complexes as countercations was applied to the synthesis of mixed vanadium-niobium POMs: $[Nb_{10}V_4O_{40}(OH)_2]^{12-}$,[69] $[H_2V_4Nb_6O_{30}]^{10-}$,[91] and a V-centered, V-capped dodecaniobate Keggin ion, $[VNb_{12}O_{40}](VO)_2]$.[70] A $[Nb_6O_{19}]$ dimer linked by Mn^{IV} and Ni^{IV} [71] and more recently Co^{III} [72] have been isolated without protective ligands bound to the transition metal, but they were initially introduced into the alkaline reaction solution with EDTA for the former and bipyridine for the latter. Both $[Nb_6O_{19}]$ and $[Ta_6O_{19}]$ have been crystallized, decorated with monovalent Mn/Re triscarbonyl species,[73] and $[Nb_6O_{19}]$ decorated with ligated Ni^{IV} has also been crystallized.[74] In many of these transition-metal decorated Lindqvist ion phases, the transition metal bonds to a face of the superoctahedal cluster with three bonds, sharing three octahedra edges. This is the same mode of bonding that is commonly observed for the alkalis (see Fig. 6).

There have been essentially no reports of uranyl peroxide clusters with open-shell transition metals, lanthanides or alkaline-earth metals as counterions, linking species, or integrated into the clusters. Like the niobates and tantalates, this synthetic chemistry is challenged by the poor solubility of these potential addenda metals in alkaline solutions in which most of these uranyl-POMs are produced. While the presence of peroxide may help aid in the solubility of some of these metals, they also create an additional challenge with redox-active metals. On the other hand, the extreme conditions of high alkalinity plus high peroxide concentration may in fact present opportunity to incorporate these metals into the uranyl POM clusters.

The tetrahedral oxoanions; PO_4^{3-}, SiO_4^{4-}, *etc.* generally reside in the center of lacunary and plenary transition-metal heteropolymetalates, whether formed in acid or alkaline conditions (see Fig. 2). While these oxoanion monomers have not yet been observed in uranyl POM clusters, methylenediphosphonate and pyrophosphate ($CH_2(PO_3)_2^{4-}$ and $P_2O_7^{4-}$ respectively) have proved quite useful serving as bridging multidentate ligands, akin the peroxide ligands.[55,75,76] Consider first the clusters containing pyrophosphate bridges, and the structurally analogous clusters containing methylenediphosphonate. The role of the pyrophosphate unit is to bridge between adjacent uranyl ions in the cluster. This is typically achieved by a "side-on" interaction between the pyrophosphate group and uranyl ion, in which one O atom of each of the two phosphate tetrahedra coordinated the uranyl ion. Two other O atoms of the phosphate tetrahedra coordinate the adjacent uranyl ion, giving the bridge. Less common is the linkage of a pyropshophate group to one uranyl ion in the "side-on" configuration, and linkage to two other uranyl ions through the sharing of one vertex each of either phosphate tetrahedron. In a single cluster, a phosphate tetrahedron that is not part of a pyrophosphate group bridges between three uranyl ions by vertex sharing. Fig. 7 provides examples of these phosphate dimer bridges in uranyl peroxide clusters; $[(UO_2)_{24}(O_2)_{24}(CH_2P_2O_6)_{12}]^{48-}$ and $[(UO_2)_{18}(O_2)_{18}(OH)_2(CH_2P_2O_6)_6(P_2O_7)_2]^{34-}$.[55] These dimer-type oxoanions are less common in transition metal POM chemistry. From transition metals POMs, diphosphonate anions have been encapsulated in molybdate clusters in particular (Fig. 7),[77,78] and the analogous disilicate anion resides in the center of polyniobate $[H_2Si_4Nb_{16}O_{56}]^{14-}$.[45]

Peroxide-ligated Nb-POMs

Nb^{5+} and Ta^{5+} form very stable bonds with peroxide O_2^{2-} ligands, and as mentioned prior, salts of $Ta(O_2)_4^{3-}$ and $Nb(O_2)_4^{3-}$ monomers are readily isolated.[18] Peroxide-ligated Nb has also

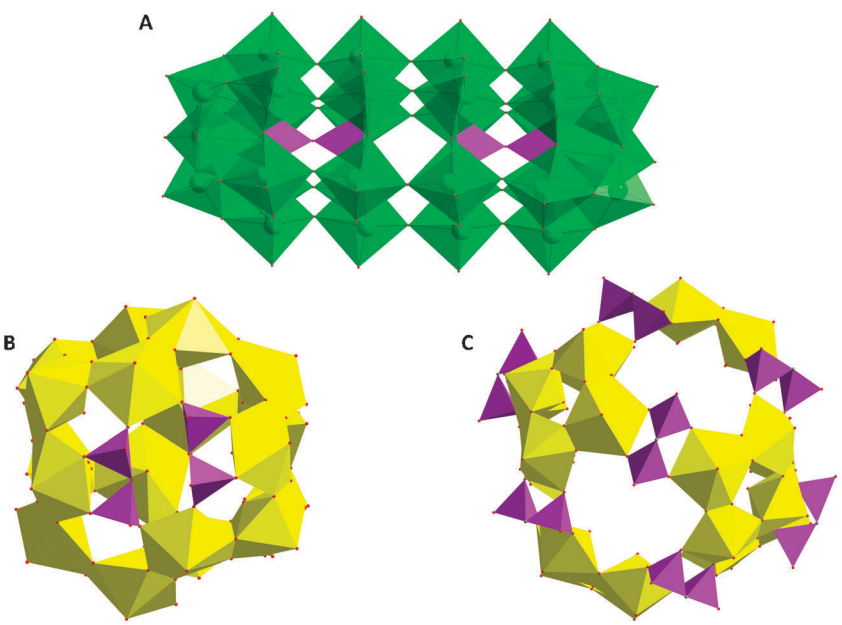

Fig. 7 Comparing phosphate dimers in transition-metal and uranyl POMs. Purple tetrahedra are the phosphate dimers (pyrophopsphate or methyldiphosphate).[78] (A) Green octahedra are molybdate in $[\{(P_2O_7)Mo_{15}O_{45}\}_2]^{8-}$. (B) $[(UO_2)_{18}(O_2)_{18}(OH)_2(CH_2P_2O_6)_6(P_2O_7)_2]^{34-}$ and (B) $[(UO_2)_{24}(O_2)_{24}(CH_2P_2O_6)_{12}]^{48-}$ (uranyl polyhedra are yellow).[55]

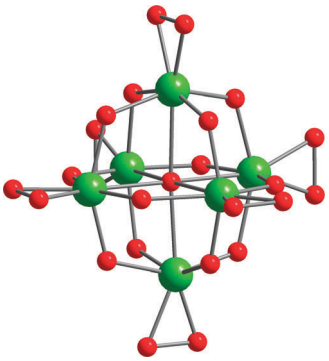

Fig. 8 View of $[Nb_6O_{13}(O_2)_6]^{8-}$ showing the different binding mode for peroxide in Nb-POMs compared to uranyl-POMs.[80] The peroxide ligand replaces the *yl*-oxygen ligand in Nb-POMs, and binds in the plane equatorial to *yl*-oxygen ligand in the uranyl-POMs (see also Fig. 1). Green spheres are Nb and red spheres are O.

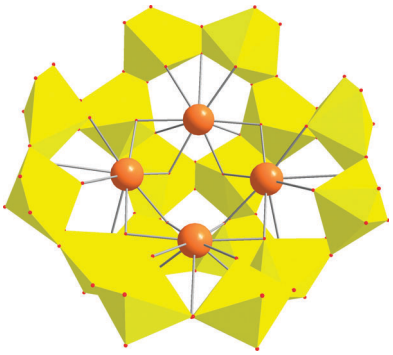

Fig. 9 View of $[(UO_2)_{16}(O_2)_{24}(OH)_8]^{24-}$ as an example of an open-shell uranyl-peroxide cluster ('lacunary-like').[22]

been isolated in the solid-state in multinuclear POMs. Examples include A-α-$[Si(NbO_2)_3W_9O_{37}]^{7-}$,[79] $[Ti_{12}Nb_6O_{38}(O_2)_6]^{10-}$,[80] and $[Nb_6O_{13}(O_2)_6]^{8-}$.[81] In all of these examples, the peroxide replaces the *yl*-oxygen of the niobium (Fig. 8); and this is quite a different mode of binding than that of the UO_2^{2+} cation where the peroxide ligands reside in the plane perpendicular to the O═U═O linear unit. Given the stability of peroxide-bonded Nb, Ta, and U, as well as the alkaline-solubility of these complexes, POM-clusters containing mixed Nb-U or Ta-U seem a tantalizing possibility. Thus far, efforts towards this goal have only produce the $Nb/Ta(O_2)_4$-centered U_{28} clusters,[15,33] but identification of the appropriate solution conditions will likely provide such clusters, again representing future potential in alkaline POM chemistry.

Lacunary transition-metal POMs and open-shell uranyl POMs

As discussed prior (also see Fig. 2), lacunary clusters and cluster derivatives are common for both the alkaline and acidic POMs. Regardless of how they form, the end result is open clusters, often described as bowl or crown shaped. They also contain unsaturated oxo ligands that both render the cluster charge more negative and provide coordination sites for dimerization, or coordinating addenda metals. Even polyniobates that are already challenged by high negative charge form these lacunary clusters, but of course the charge is always mitigated by bonded cations, such as the PO_2^+-decorated A-type trivacant α-Keggin $[(PO_2)_3PNb_9O_{34}]^{15-}$.[82] There are also examples of uranyl POMs that assemble into open cluster structures, much like the transition-metal POMs. These include $[(UO_2)_{32}(O_2)_{40}(OH)_{24}]^{40-}$,[83] $[(UO_2)_{16}(O_2)_{24}(OH)_8]^{24-}$, $[(UO_2)_{20}(OH)_{16}(O_2)_{28}]^{32-}$ and $[(UO_2)_{24}(O_2)_{36}(OH)_{12}]^{36-}$;[22] and the U_{16} cluster is shown in Fig. 9 as examples. These always feature unshared peroxide edges of the uranyl polyhedral, and like the closed capsules, they are 'filled' with alkali-cations and water molecules. We described earlier in the manuscript the process to obtain lacunary clusters from the acid-side of POMs: by increasing the pH of a solution of POMs, controlled disassembly can provide isolation of cluster fragments, or lacunary clusters. The alkaline-side has produced lacunary derivatives, but distinct and controllable synthesis conditions have not been prescribed. This seems to be consistent with the uranyl POM clusters: no distinct solution chemistry is identified that controls the formation of plenary *vs.* lacunary cluster geometries.

Alkaline and acidic exceptions in POM chemistry

While recognizing trends and establishing rules is important in understanding and controlling synthetic chemistry, there are always some exceptions. The acidic and basic sides of polyoxometalates were largely defined empirically in ambient, aqueous chemistries; yet later hydrothermal synthesis provided a great deal to the development of the alkaline Nb-POMs.[45] Likewise, hydrothermal and solvothermal synthesis has provided an alkaline-side to the POM chemistry of vanadium. Like group V Nb^{5+} and Ta^{5+}, V^{5+} also forms highly charged clusters; and therefore like Nb-POMs; V-POMs tend to be linked into frameworks or are capped to mitigate the high charge.[84] However, it has the smallest ionic radius of the POM-forming metals, and its ambient aqueous chemistry is more akin to that of Mo and W: monomeric in alkaline conditions and forming clusters upon acidification. Hydrothermal/solvothermal synthesis of vanadate POMs in alkaline pH solutions containing amines or metal amine complexes has been recognized; see for instance Tripathi *et al.*[85]

A total of 38 uranyl POM clusters have been reported. In most cases the synthetic details reported included the pH of the solution from which the clusters assembled and crystallized. The clusters are collected in Fig. 10, where they are plotted on the basis of their mother solution pH and the number of uranyl ions in solution. From this plot, it is apparent that cage clusters consisting of uranyl peroxide polyhedral can form in aqueous solution over the pH range of about 4 to 13. Those clusters that are built from uranyl ions that are only bridged by hydroxyl and/or peroxo groups generally form in alkaline solutions, with most in solutions of pH-9 or greater. The exceptions are U_{44}, which crystallizes from a solution with pH = 6.7, and U_{42} which grew from solution with pH = 7.9.[75,86] The smaller cage clusters, built from 30 or fewer uranyl ions, formed from solutions with a pH of at least 10.5. In contrast, the largest cluster with 60 uranyl ions formed at pH = 9. Note that the mineral studtite, $[(UO_2)(O_2)(H_2O)_2](H_2O)_2$, is insoluble in acidic conditions,

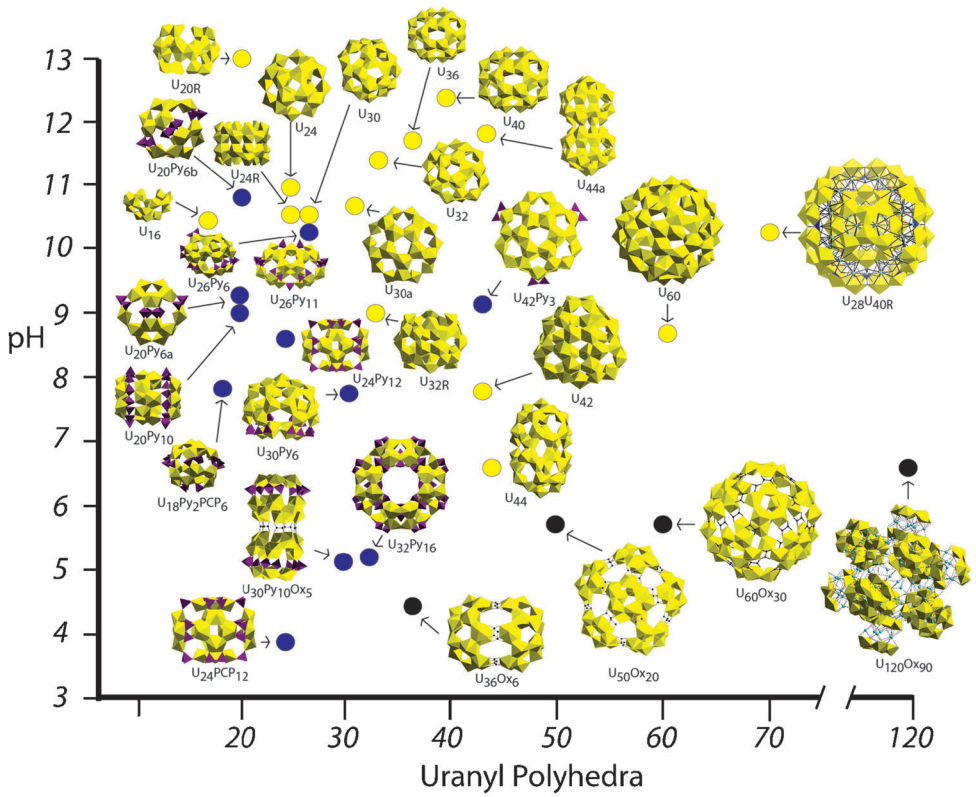

Fig. 10 Urany-POM cluster as a function of pH of crystallization. Yellow dots mean clusters containing uranyl triperoxide and/or uranyl diperoxidedihydroxide polyhedra only; black dots mean clusters containing also oxalate ligands; blue dots mean clusters containing also diphosphate and/or methyldiphosphonate polyhedra.

and the combination of uranyl and peroxide under acidic conditions results in its immediate precipitation, rather than formation of cages. However, where other means of bridging uranyl ions are provided, such as pyrophosphate or oxalate, cage clusters readily self-assemble under acidic conditions and studtite generally does not precipitate. Cage clusters containing oxalate bridges only have been reported from acidic solutions, with oxalic acid providing the oxalate. In contrast, although pyrophosphoric acid is used as a source of phosphate in uranyl cluster assembly; a base is typically added as well, and it is possible to synthesize clusters of uranyl polyhedral that include pyrophosphate bridges over a broad range of pH, from about 4 to 11.

The initial manuscript that reported synthesis of uranyl peroxide cage clusters that included pyrophosphate and/or methylenediphosphonate bridges provided the solution pH range over which clusters were crystallized.[55] Some clusters were crystallized over a very limited pH range, whereas others, such as $U_{24}PCP_{12}$, (PCP = dimethylphosphonate) crystallized over the range of 4.0 to 9.1. In comparison, the cluster $U_{24}Py_{12}$ (Py = pyrophosphate), which is structurally identical to $U_{24}PCP_{12}$ but with pyrophosphate replacing the methylenediphosphonate bridges, formed from solution with pH = 7.2–10. Most of the uranyl pyrophosphate clusters reported contain only pyrophosphate and peroxide bridges between uranyl ions, although two also contain some hydroxyl bridges ($U_{18}Py_2PCP_6$[55] and $U_{42}Py_3$[75]). As discussed above, neither the peroxide ligands nor the *yl*-oxygen ligands are expected to be susceptible to protonation. In contrast, the pyrophosphate group that bridges two uranyl ions has four oxo-ligands that are terminal. These are potentially protonated in some cases, especially in the case of the clusters synthesized under acidic conditions. The availability of these oxo-ligands for protonation may help to explain the broad pH range in which uranyl pyrophosphate clusters form.

Where transition metal and actinde POM chemistry meet

As discussed prior, synthesis of mixed niobate-uranyl peroxide clusters in alkaline conditions has not yet proved fruitful. Perhaps this is due to the different binding modes of Nb^{5+} and U^{6+} to peroxide in aqueous alkaline conditions: the peroxide replaces the *yl*-oxygen on Nb, and bonds perpendicular to the *yl*-oxygen on U. However, UO_2^{2+} combined with tungstate POMs has produced clusters featuring up to twelve UO_2 moieties sandwiched between lacunary fragments.[87,88] The chemical strategy to produce these compounds is similar to that of the numerous transition metal and lanthanide tungstate lacunary derivatives, where the lacunary fragments serve as inorganic ligands to actinyl monomers or small polynuclear assemblies. Kortz[89] produced one noteworthy assembly in which two uranyl peroxide square rings (hosting a Li^+ cation) reside inside a curved lacunary phosphotungstate ('P_6W_{36}') fragment. Each uranyl has two *cis*-peroxide ligands, perpendicular to the linear UO_2, and then two bonds to the oxo ligands of the phosphotungstate POM. This is the same

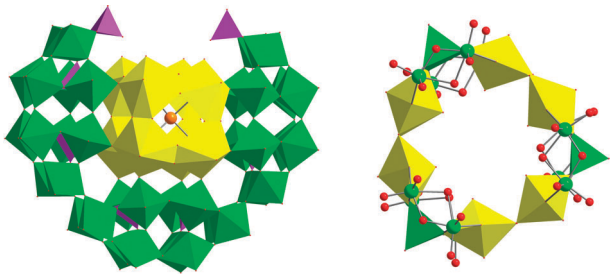

Fig. 11 Hybrid uranyl-tungstate POM clusters. Left: lacunary phosphotungstate hosting two uranyl triperoxide square rings.[89] Right: 9-member edge-sharing ring of alternating uranyl hexagonal bipyramid dimers and tungstate square pyramids (polyhedral representation), and also decorated with edge-sharing tungstate octahedra (ball-and-stick).[90] Green is tungstate, purple is phosphate, yellow is uranyl and orange sphere is Li inside the uranyl peroxide square ring.

square building block observed in the very symmetric U_{24} or Np_{24} clusters,[1] where two *cis*-OH ligands are replaced by the POM oxo ligands—see Fig. 11 and also Fig. 4.

Recently, a mixed W-U POM was reported with composition $\{[W_5O_{21}]_3[(U^{VI}O_2)_2(\mu\text{-}O_2)]_3\}^{30-}$.[90] (Fig. 11) Pairs of uranyl ions are bridged through peroxide groups, and each uranyl ion is further coordinated by the oxo ligands of the W^{6+} cations. There are three resulting dimers of uranyl peroxide polyhedra that are distributed about the circumference of a crown structure. The uranyl polyhedra are linked into the cluster through groups of five W^{6+} cations present as $[W_5O_{21}]^{12-}$ fragments. The W cations are coordinated by either five or six oxo ligands, with typical POM W–O bond lengths ranging from 1.69 to 2.42 Å. BVS sums for the oxo ligands of the cluster indicated several have sums that are well below their formal valence, and this may be due to protonation and/or bonds to Na or Li cations that were not located in the structure determination. The synthesis solution for this cluster was typical of many of the alkaline-peroxide-uranyl cluster syntheses: high hydroxide, high peroxide concentration. In addition, phosphotungstic acid ($H_3PW_{12}O_{40}$ Keggin ion) was utilized as a W-precursor; which typically breaks down to monomers under such alkaline conditions. The tungstate monomer form, not unlike the pyrophosphate, apparently presents a suitable geometry for bridging uranyl peroxide building blocks, allowing assembly of this truly integrated tugstate-uranyl POM.

Conclusions

Over the last seven years, the chemistry of actinyl POMs has been realized and has expanded, bringing forth frequent and surprising new discoveries each subsequent year; and this paper represents the first thorough comparison of this new class of POMs with the transition-metal POMs. We began the process of this tutorial review with the bias that these uranyl peroxide based POM clusters are more akin to the alkaline-side of POM chemistry. This bias was due to the fact that they both self-assemble and are stable in aqueous base, while aqueous acid results in precipitation of related oxide phases. Further, the alkaline transition-metals, Ta and Nb, form stable bonds with peroxide, as does uranium. However, this review has unearthed as many similarities with the acidic POMs as alkaline POMs: in particular, the ability to isolate stable uranyl peroxide monomer forms, the assembly of uranyl peroxide clusters in acidic solution if the appropriate ligands are present, and the solubility trends with alkali counterions. The charge-densities of the uranyl POMs are similar to that of the alkaline POMs if the encapsulated species are not considered, but more akin to the acidic POMs if these species are accounted for. Finally, the hybrid W-uranyl POMs have been realized, while related Nb-uranyl POMs remain a challenge. By comparing the fledging chemistry of the uranyl POMs to that of the well-studied transition-metal POMs, we recognize many opportunities for the future with the uranyl POMs including non-aqueous chemistry, understanding solution behavior, and assembly of clusters that incorporate other addenda metals including rare-earths, open-shell transition metals and alkaline earths. This review has brought forth considerable optimism and excitement that much remains to be discovered in the solid-state and solution chemistry of uranyl peroxide POMs.

Acknowledgements

This work was supported as part of the Materials Science of Actinides, an Energy Frontier Research Center funded by the Department of Energy, Office of Science, Office of Basic Energy Sciences under award number DE-SC0001089. Sandia National Laboratories is a multiprogram laboratory operated by Sandia Corporation, a wholly owned subsidiary of Lockheed Martin company, for the Department of Energy's National Nuclear SecurityAdministration under contract DE-AC04-94AL85000.

References

1 P. C. Burns, K. A. Kubatko, G. Sigmon, B. J. Fryer, J. E. Gagnon, M. R. Antonio and L. Soderholm, *Angew. Chem., Int. Ed.*, 2005, **44**, 2135–2139.
2 M. Kunz and I. D. Brown, *J. Solid State Chem.*, 1995, **115**, 395–406.
3 H. T. Evans and J. A. Konnert, *Am. Mineral.*, 1978, **63**, 863–868.
4 A. Kobayashi and Y. Sasaki, *Chem. Lett.*, 1975, 1123–1124.
5 J. J. Cruywagen, *Adv. Inorg. Chem.*, 2000, **49**, 127–182.
6 R. G. Denning, *J. Phys. Chem. A*, 2007, **111**, 4125–4143.
7 T. J. R. Weakley, H. T. Evans, J. S. Showell, G. F. Tourne and C. M. Tourne, *J. Chem. Soc., Chem. Commun.*, 1973, 139–140.
8 M. Nyman, *Dalton Trans.*, 2011, **40**, 8049–8058.
9 B. Vlaisavljevich, L. Gagliardi and P. C. Burns, *J. Am. Chem. Soc.*, 2010, **132**, 14503–14508.
10 P. C. Burns, *Mineral. Mag.*, 2011, **75**, 1–25.
11 P. Miro, S. Pierrefixe, M. Gicquel, A. Gil and C. Bo, *J. Am. Chem. Soc.*, 2010, **132**, 17787–17794.
12 F. Clarens, J. de Pablo, I. Casas, J. Gimenez, M. Rovira, J. Merino, E. Cera, J. Bruno, J. Quinones and A. Martinez-Esparza, *J. Nucl. Mater.*, 2005, **345**, 225–231.
13 N. W. Alcock, *J. Chem. Soc. A*, 1968, 1588.
14 M. Nyman, M. A. Rodriguez and C. F. Campana, *Inorg. Chem.*, 2010, **49**, 7748–7755.
15 M. Nyman, M. A. Rodriguez and T. M. Alam, *Eur. J. Inorg. Chem.*, 2011, 2197–2205.
16 C. R. Armstrong, M. Nyman, T. Shvareva, G. E. Sigmon, P. C. Burns and A. Navrotsky, *Proc. Natl. Acad. Sci. U. S. A.*, 2012, **109**, 1874–1877.
17 R. A. Zehnder, E. R. Batista, B. L. Scott, S. M. Peper, G. S. Goff and W. H. Runde, *Radiochim. Acta*, 2008, **96**, 575–578.

18 H. Hartl, F. Pickhard, F. Emmerling and C. Rohr, *Z. Anorg. Allg. Chem.*, 2001, **627**, 2630–2638.
19 T. M. Anderson, M. A. Rodriguez, F. Bonhomme, J. N. Bixler, T. M. Alam and M. Nyman, *Dalton Trans.*, 2007, 4517–4522.
20 G. E. Sigmon, D. K. Unruh, J. Ling, B. Weaver, M. Ward, L. Pressprich, A. Simonetti and P. C. Burns, *Angew. Chem., Int. Ed.*, 2009, **48**, 2737–2740.
21 G. E. Sigmon, J. Ling, D. K. Unruh, L. Moore-Shay, M. Ward, B. Weaver and P. C. Burns, *J. Am. Chem. Soc.*, 2009, **131**, 16648.
22 G. E. Sigmon, B. Weaver, K. A. Kubatko and P. C. Burns, *Inorg. Chem.*, 2009, **48**, 10907–10909.
23 T. Akutagawa, D. Endo, S. I. Noro, L. Cronin and T. Nakamura, *Coord. Chem. Rev.*, 2007, **251**, 2547–2561.
24 M. H. Alizadeh, S. P. Harmalker, Y. Jeannin, J. Martinfrere and M. T. Pope, *J. Am. Chem. Soc.*, 1985, **107**, 2662–2669.
25 M. H. Chiang, M. R. Antonio and L. Soderholm, *Dalton Trans.*, 2004, 3562–3567.
26 A. Yoshida, Y. Nakagawa, K. Uehara, S. Hikichi and N. Mizuno, *Angew. Chem., Int. Ed.*, 2009, **48**, 7055–7058.
27 P. Roman, A. S. Jose, A. Luque and J. M. Gutierrezzorrilla, *Inorg. Chem.*, 1993, **32**, 775–776.
28 S. Inami, M. Nishio, Y. Hayashi, K. Isobe, H. Kameda and T. Shimoda, *Eur. J. Inorg. Chem.*, 2009, 5253–5258.
29 T. Kurata, A. Uehara, Y. Hayashi and K. Isobe, *Inorg. Chem.*, 2005, **44**, 2524–2530.
30 A. Muller, E. Krickemeyer, J. Meyer, H. Bogge, F. Peters, W. Plass, E. Diemann, S. Dillinger, F. Nonnenbruch, M. Randerath and C. Menke, *Angew. Chem., Int. Ed. Engl.*, 1995, **34**, 2122–2124.
31 A. Ziv, A. Grego, S. Kopilevich, L. Zeiri, P. Miro, C. Bo, A. Muller and I. A. Weinstock, *J. Am. Chem. Soc.*, 2009, **131**, 6380.
32 O. Petina, D. Rehder, E. T. K. Haupt, A. Grego, I. A. Weinstock, A. Merca, H. Bogge, J. Szakacs and A. Muller, *Angew. Chem., Int. Ed.*, 2011, **50**, 410–414.
33 A. Gil, D. Karhanek, P. Miro, M. R. Antonio, M. Nyman and C. Bo, *Chem.–Eur. J.*, 2012, in press.
34 P. C. Yin, D. Li and T. B. Liu, *Isr. J. Chem.*, 2011, **51**, 191–204.
35 Y. F. Wang, A. Neyman, E. Arkhangelsky, V. Gitis, L. Meshi and I. A. Weinstock, *J. Am. Chem. Soc.*, 2009, **131**, 17412–17422.
36 R. Bakri, A. Booth, G. Harle, P. S. Middleton, C. Wills, W. Clegg, R. W. Harrington and R. J. Errington, *Chem. Commun.*, 2012, **48**, 2779–2781.
37 J. Ettedgui, Y. Diskin-Posner, L. Weiner and R. Neumann, *J. Am. Chem. Soc.*, 2011, **133**, 188–190.
38 M. R. Antonio, M. Nyman and T. M. Anderson, *Angew. Chem., Int. Ed.*, 2009, **48**, 6136–6140.
39 E. M. Villa, C. A. Ohlin, E. Balogh, T. M. Anderson, M. D. Nyman and W. H. Casey, *Angew. Chem., Int. Ed.*, 2008, **47**, 4844–4846.
40 M. Matsumoto, Y. Ozawa and A. Yagasaki, *Polyhedron*, 2010, **29**, 2196–2201.
41 M. Matsumoto, Y. Ozawa and A. Yagasaki, *Inorg. Chem. Commun.*, 2011, **14**, 115–117.
42 T. M. Anderson, S. G. Thoma, F. Bonhomme, M. A. Rodriguez, H. Park, J. B. Parise, T. M. Alam, J. P. Larentzos and M. Nyman, *Cryst. Growth Des.*, 2007, **7**, 719–723.
43 M. Nyman, T. M. Alam, F. Bonhomme, M. A. Rodriguez, C. S. Frazer and M. E. Welk, *J. Cluster Sci.*, 2006, **17**, 197–219.
44 M. Nyman, F. Bonhomme, T. M. Alam, J. B. Parise and G. M. B. Vaughan, *Angew. Chem., Int. Ed.*, 2004, **43**, 2787–2792.
45 M. Nyman, F. Bonhomme, T. M. Alam, M. A. Rodriguez, B. R. Cherry, J. L. Krumhansl, T. M. Nenoff and A. M. Sattler, *Science*, 2002, **297**, 996–998.
46 Y. Hou, M. Nyman and M. A. Rodriguez, *Angew. Chem., Int. Ed.*, 2011, **50**, 12514–12517.
47 E. Balogh, T. M. Anderson, J. R. Rustad, M. Nyman and W. H. Casey, *Inorg. Chem.*, 2007, **46**, 7032–7039.
48 V. W. Day, W. G. Klemperer and D. J. Maltbie, *J. Am. Chem. Soc.*, 1987, **109**, 2991–3002.
49 T. Ozeki, T. Yamase, H. Naruke and Y. Sasaki, *Bull. Chem. Soc. Jpn.*, 1994, **67**, 3249–3253.
50 R. P. Bontchev, E. L. Venturini and M. Nyman, *Inorg. Chem.*, 2007, **46**, 4483–4491.
51 R. P. Bontchev and M. Nyman, *Angew. Chem., Int. Ed.*, 2006, **45**, 6670–6672.
52 S. Zhang, J. Zhao, P. Ma, H. Chen, J. Niu and J. Wang, *Cryst. Growth. Des.*, 2012, ASAP.
53 D. L. Long, P. Kögerler, A. D. C. Parenty, J. Fielden and L. Cronin, *Angew. Chem., Int. Ed.*, 2006, **45**, 4798–4803.
54 J. Yan, J. Gao, D. L. Long, H. N. Miras and L. Cronin, *J. Am. Chem. Soc.*, 2010, **132**, 11410–11411.
55 J. Ling, J. Qiu, G. E. Sigmon, M. Ward, J. E. S. Szymanowski and P. C. Burns, *J. Am. Chem. Soc.*, 2010, **132**, 13395–13402.
56 S. Ganapathy, M. Fournier, J. F. Paul, L. Delevoye, M. Guelton and J. P. Amoureux, *J. Am. Chem. Soc.*, 2002, **124**, 7821–7828.
57 J. R. Black, M. Nyman and W. H. Casey, *Geochim. Cosmochim. Acta*, 2006, **70**, A53–A53.
58 E. M. Villa, C. A. Ohlin and W. H. Casey, *J. Am. Chem. Soc.*, 2010, **132**, 5264–5272.
59 R. K. Murmann and K. C. Giese, *Inorg. Chem.*, 1978, **17**, 1160–1166.
60 M. Filowitz, W. G. Klemperer, L. Messerle and W. Shum, *J. Am. Chem. Soc.*, 1976, **98**, 2345–2346.
61 J. R. Rustad and W. H. Casey, *Nat. Mater.*, 2012.
62 Z. Szabo and I. Grenthe, *Inorg. Chem.*, 2010, **49**, 4928–4933.
63 C. L. Hill, *J. Mol. Catal. A: Chem.*, 2007, **262**, 2–6.
64 Y. Lu, Y. Xu, Y. G. Li, E. B. Wang, X. X. Xu and Y. Ma, *Inorg. Chem.*, 2006, **45**, 2055–2060.
65 M. H. Chiang, M. R. Antonio, C. W. Williams and L. Soderholm, *Dalton Trans.*, 2004, 801–806.
66 G. Chen, C. Z. Wang, P. T. Ma, J. P. Wang and J. Y. Niu, *J. Cluster Sci.*, 2010, **21**, 121–131.
67 J. P. Wang, H. Y. Niu and J. Y. Niu, *J. Chem. Sci.*, 2008, **120**, 309–313.
68 J. Y. Niu, G. Chen, J. W. Zhao, P. T. Ma, S. Z. Li, J. P. Wang, M. X. Li, Y. Bai and B. S. Ji, *Chem.–Eur. J.*, 2010, **16**, 7082–7086.
69 P. Huang, C. Qin, X. L. Wang, C. Y. Sun, G. S. Yang, K. Z. Shao, Y. Q. Jiao, K. Zhou and Z. M. Su, *Chem. Commun.*, 2012, **48**, 103–105.
70 G. L. Guo, Y. Q. Xu, J. Cao and C. W. Hu, *Chem. Commun.*, 2011, **47**, 9411–9413.
71 C. M. Flynn and G. D. Stucky, *Inorg. Chem.*, 1969, **8**, 332.
72 P. T. Ma, G. Chen, G. Wang and J. P. Wang, *Russ. J. Coord. Chem.*, 2011, **37**, 772–775.
73 M. H. Dickman and M. T. Pope, *Inorg. Chem.*, 2001, **40**, 2582–2586.
74 G. Chen, P. T. Ma, J. P. Wang and J. Y. Niu, *J. Coord. Chem.*, 2010, **63**, 3753–3763.
75 D. K. Unruh, J. Ling, J. Qiu, L. Pressprich, M. Baranay, M. Ward and P. C. Burns, *Inorg. Chem.*, 2011, **50**, 5509–5516.
76 J. Ling, J. Qiu, J. E. S. Szymanowski and P. C. Burns, *Chem.–Eur. J.*, 2011, **17**, 2571–2574.
77 S. Himeno, N. Inazuma and E. Kitano, *J. Sep. Sci.*, 2007, **30**, 1077–1081.
78 U. Kortz, *Inorg. Chem.*, 2000, **39**, 623–624.
79 G. S. Kim, H. D. Zeng and C. L. Hill, *Bull. Korean Chem. Soc.*, 2003, **24**, 1005–1008.
80 C. A. Ohlin, E. M. Villa, J. C. Fettinger and W. H. Casey, *Inorg. Chim. Acta*, 2010, **363**, 4405–4407.
81 C. A. Ohlin, E. M. Villa, J. C. Fettinger and W. H. Casey, *Angew. Chem., Int. Ed.*, 2008, **47**, 8251–8254.
82 M. Nyman, A. J. Celestian, J. B. Parise, G. P. Holland and T. M. Alam, *Inorg. Chem.*, 2006, **45**, 1043–1052.
83 G. E. Sigmon and P. C. Burns, *J. Am. Chem. Soc.*, 2011, **133**, 9137–9139.
84 M. I. Khan, E. Yohannes and R. J. Doedens, *Angew. Chem., Int. Ed.*, 1999, **38**, 1292–1294.
85 A. Tripathi, T. Hughbanks and A. Clearfield, *J. Am. Chem. Soc.*, 2003, **125**, 10528–10529.
86 D. K. Unruh, A. Burtner, L. Pressprich, G. E. Sigmon and P. C. Burns, *Dalton Trans.*, 2010, **39**, 5807–5813.
87 A. J. Gaunt, I. May, R. Copping, A. I. Bhatt, D. Collison, O. D. Fox, K. T. Holman and M. T. Pope, *Dalton Trans.*, 2003, 3009–3014.
88 M. Mohadeszadeh, *J. Cluster Sci.*, 2011, **22**, 183–192.
89 S. S. Mal, M. H. Dickman and U. Kortz, *Chem.–Eur. J.*, 2008, **14**, 9851–9855.
90 P. Miro, J. Ling, J. Qiu, P. C. Burns, L. Gagliardi and C. J. Cramer, *Inorg. Chem.*, 2012, in review.
91 G. Guo, Y. Xu and J. Cao, *et al.*, *Chem.–Eur. J.*, 2012, **18**, 3493–3497.